

ZVZCS Based High Frequency Link Grid Connected SVM Applied Three Phase Three Level Diode Clamped Inverter for Photovoltaic Applications Part-II

Soumyadeep Ray, Madichetty Sreedhar, Abhijit Dasgupta
School of Electrical Engineering, KIIT University, India

Article Info

Article history:

Received Dec 19, 2013
Revised May 21, 2014
Accepted Jun 1, 2014

Keyword:

Diode Clamped Inverter
High Frequency Link
Minority Charge Carrier
Inspired Algorithm
SVPWM
ZVS ZCS Converter

ABSTRACT

This article proposes a newly proposed highly effective Zero Voltage and Zero Current switching based Front end converter with a High Frequency Transformer with a Three Phase Three Level Diode Clamped Inverter in photovoltaic applications. The switching scheme is implemented in MATLAB/ Simulink condition. ZVZCS condition is achieved. This type of converter shows high efficiency and very negligible switching loss. Finally ZVZCS based High Frequency Link Diode Clamped Inverter is connected to Grid. An MCI optimized Current controller is used with SVM switching technique. In This article, responses with three types of controllers (I, PI, PID) have been examined and compared. Simulation results show the effectiveness, and validity of this technique.

Copyright © 2014 Institute of Advanced Engineering and Science.
All rights reserved.

Corresponding Author:

Soumyadeep Ray,
School of Electrical Engineering,
KIIT University, India
Email: write2prithu@gmail.com

1. INTRODUCTION

Solar energy is becoming popular from previous days. Mainly Two types of solar energy systems are present. Stand alone system and Grid connected system is proposed in Literature. Grid connected Photovoltaic(PV) system does not require bulk battery. The work on PV generation systems, like PV array connected through first boost converter and Three Phase Inverter to the grid, has increased in the last decade due to the rise in demand for electric power. With the advancement of the power electronics converters mainly the DC-DC converters and three phase inverters, this generated power can be utilized and supplied to grid. Inverter efficiency needs to be improved in order to mitigate the losses, photovoltaic module's low efficiency. Many researchers have proposed various topologies and different control theories for three phase grid connected photovoltaic system.[1-10] Advantages which are motivating grid connected photovoltaic applications are Reduction of costs of PV panel; Operation does not pollute the environment. Figure 1 shows the conventional procedure of connecting photovoltaic system to the grid.



Figure 1. Conventional PV system connected to Grid

Multi Level Diode Clamped Inverter has been proposed and accepted for applications in Medium and High power drives and the utility systems. As compared with the other multi-level converter topologies the Diode Clamped converter uses a very less number of capacitors and switches in order to get the desired output voltage level. It is therefore more economical and reliable. [11]-[17]. Hence, it is combining the best possible two techniques and makes the system much more efficient.

In the above system Stability of the power system was modeled and analysed, Total Harmonic Distortion (THD) should be minimum, Lower Order Harmonics should be minimum. The total set up size should be small, Inverter efficiency should be high.

In addition it is also important that the inverter needs to operate very quickly and a high frequency operation while generating PWM signals with minimum losses. Hence, the controller plays a vital role.

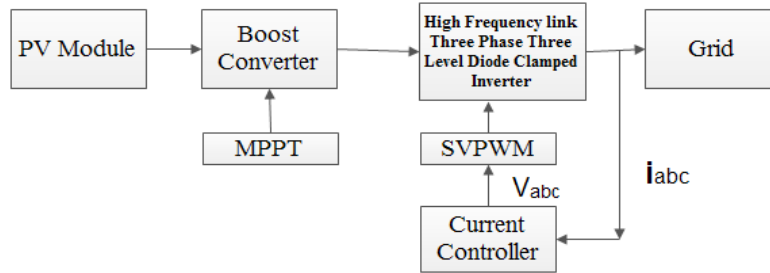


Figure 2. Proposed PV system connected with Grid

In order to achieve Less set up size, less total harmonic distortion, less lower Order Harmonics without compromising efficiency a new technique is already proposed [18]-[28]. In this paper Grid connected ZVZCS based Three Level Three Phase Diode Clamped Inverter [29], [30] is proposed with an optimized current controller. In this paper SVPWM technique is used in order to minimize switching loss in the Final Inverter. Grid connected ZVZCS based Inverter is implemented in MATLAB/ Simulink condition and results show the effectiveness of the technique along with Grid Voltage and Current.

2. P AND O MPPT

The Photovoltaic system has some major disadvantages, the conversion and generation of Power, till now, is not efficient and power changes with varying insolation and temperature. Power-Voltage and Current- voltage relationship is non linear in nature. So a unique point is present in Power- Voltage curve or in Current-Voltage Curve called Maximum Power point, at which point that module operates with maximum efficiency at particular weather condition. The exact value of Maximum power point is not fixed, but can be found by using search type algorithms. Mainly Incremental conductance and Perturb and Observe(P and O) MPPT algorithms are used. P and O MPPT algorithm is simple for implementation purpose. Figure 3 shows P and O MPPT algorithm.

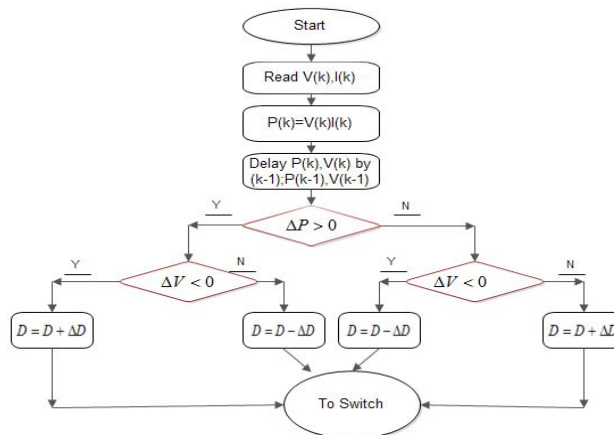


Figure 3. P and O MPPT Algorithm

This algorithm is based on the calculation of output power of PV module and power is changed by current and voltage. The algorithm calculate the value of power at k th instant and at $(k+1)$ th instant and difference is calculated. If the magnitude of the power is increasing in nature, the perturbation will continue in the same direction in the next cycle, otherwise reversed. At MPP, in order to reduce oscillation, the perturbation step size should be minimized.

Figure 4 shows the voltage, current and power waveforms for PV systems with MPPT, in constant irradiation (800 W/m^2) and constant temperature (50°C).

So, PV module is connected to Boost Converter where switching is done by following MPPT algorithm.

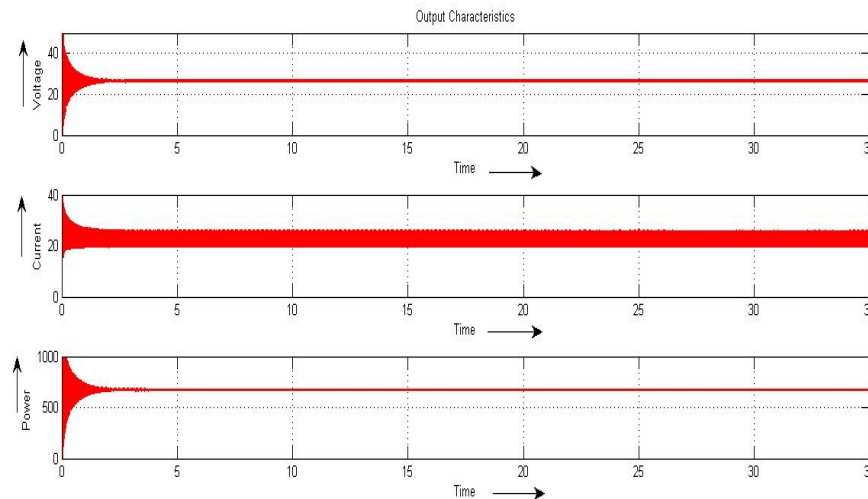


Figure 4. Power, voltage and current characteristics of PV module with MPPT in a constant temperature and constant irradiation

3. HIGH FREQUENCY LINK THREE LEVEL THREE PHASE DIODE CLAMPED INVERTER - BASIC PRINCIPLE AND OPERATION

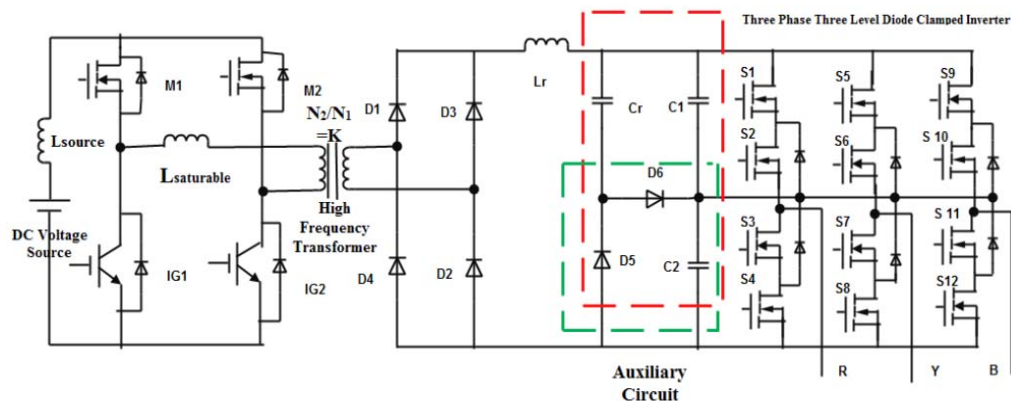


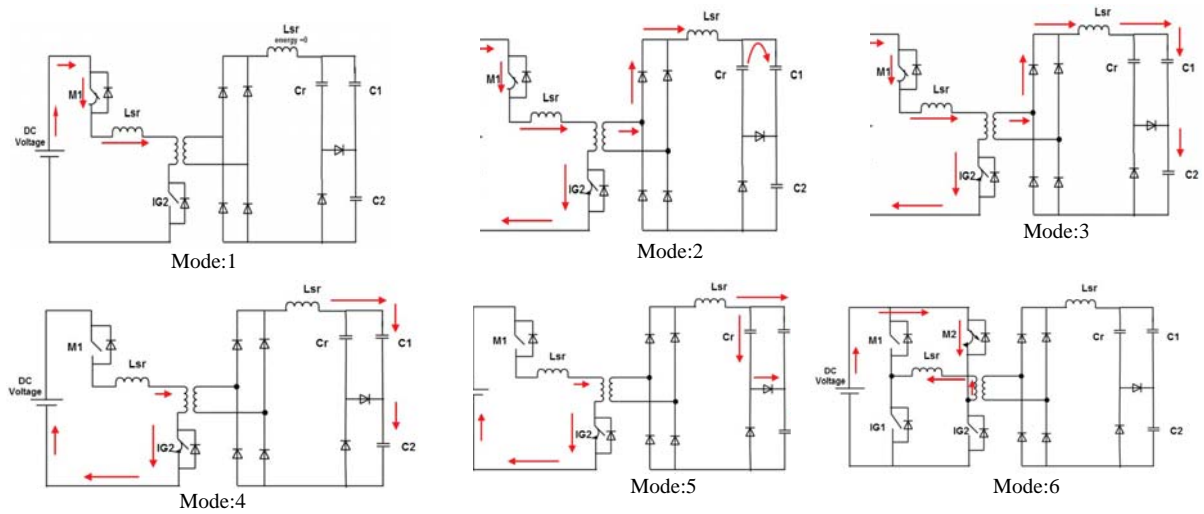
Figure 5. High Frequency Link Diode Clamped Three level Three Phase Inverter

The numbering order of switches is M1, M2, IG1, IG2 and D1, D2, D3, D4 and S1, S2, S3, S4, S5, S6. The dc bus consists of two capacitors C1, C2. The voltage across each capacitor is $V_{dc}/2$. An m -level inverter leg requires $(m-1)$ capacitors, $2(m-1)$ switching devices and $(m-1)(m-2)$ clamping diodes [31]. The input supply from any fuel cell can be given to the inverter which consists of a two legs called leading leg and lagging leg. Both leg consists of a MOSFET and IGBT indicated as M1, IG1, M2, IG2 respectively. The out put of the inverter from high frequency transformer along with an inductor L_{Source} . The pulsating output

is given to the diode bridge rectifier for which the capacitor, inductor will acts as an input filter, blocking capacitor as well. The green dotted line will acts as filter and combination of green dotted and red dotted line indicates as auxiliary circuit. The main function of this auxiliary circuit is to ensure the ZCS and ZVS for the front end inverter. L_{sr} is the saturable reactor which is in placed series with the high frequency transformer, I_{Lsr} is the current passing through the reactor, I_{PTrans} , I_{Strans} , V_{Ptrans} , V_{Strans} is the current and voltage of the tranfomrer primary and secondary respectively. I_{lo} is the current passing through the filter cum auxiliary inductor, I_{da} is the current passing through the auxilay diode. The proposed circuit is shown Figure 5.

This principle can be explained in two sections. In the first, the basic principle and operation of a front end isolated inverter and three phase three level diode clamped inverter in the second. The basic operation of the proposed ZVZCS converter have fourteen operating modes and working on the principle of pulse phase shift modulation technique. Here, it has been considered only six operating modes for the positive half cycle and remaining will be reflected of these modes.

Mode1: ($0 < t < t_1$): Here assumed that, the inductor is in discharged condition. When the switch M1 is on condition, the total energy that is present in inductor dissipated and current in this condition is zero.



Mode2: ($t_1 < t < t_2$): In this mode, both switches M1 and IG2 are in on. The total input power will be transferred through the transformer to output. Here at this time the filter capacitor C is charged along with the filter inductor. The amount of energy that can be stored at this time in inductor is $\frac{1}{2}LI^2$ and in capacitor is $\frac{1}{2}CV^2$.

The current through the transformer is given in Equation (1).

$$I_{tr}(t) = N \cdot I_0 (1 - \cos(\omega t)) - \frac{V_s - V_0}{Z} \frac{1}{N} \sin(\omega t) + NI_0 \quad (1)$$

$$I_C(t) = NI_0 - I_{tr}(t) \quad (2)$$

$$V_C(t) = NV_{in}(1 - \cos(\omega t)) - N^2ZI_0 \sin(\omega t) \quad (3)$$

Mode 3: ($t_2 < t < t_3$): This mode begins with auxiliary circuit which is shown in red dotted lines, The capacitor is slowly charging. Since the capacitor voltage V_{ca} is less than the input voltage, current will start flowing through auxiliary circuit which is shown in Figure 2. M1 turns on softly as inductor L_r is in series with this switch and limits the rise in current through it. C_r discharges into the auxiliary inductor during this mode. Since voltage V_{cs} is lesser than the bridge voltage, diode D1 is reversed biased and does not conduct. This mode ends when C_r voltage reaches the voltage across off-state bridge switches.

Mode 4: ($t_4 < t < t_5$): This mode begins when diode D1 becomes forward biased and starts to conduct. The voltage across the bridge switches therefore follows capacitor voltage V_{ca} which is decreasing. This voltage is also equal to the voltage across the transformer. Ideally, if the voltage across the transformer is less than the output. Diodes become reversed biased and power is not transferred to the output, but this power transfer does not in fact stop immediately because of the presence of leakage inductance in the transformer. The transformer current reaches zero at the end of this mode.

$$V_{ab} = \frac{NI_0}{\omega} \left(\frac{1}{\omega^2} - \frac{1}{c_{tot}} \right) \sin(\omega t) - \frac{NI_0}{\omega^2} T + 2V_{in} \quad (4)$$

$$I_{tran} = NI \left(1 - \frac{c}{\omega^2} \right) \cos(\omega t) + \frac{c}{\omega^2} NI_0 \quad (5)$$

$$V_c = \frac{I_0}{c_{tot}\omega^2} \sin(\omega t) + \frac{I_0}{c_{tot}\omega^2} \sin(\omega t) - NV_0 \quad (6)$$

Mode 5: ($t_5 < t < t_6$): The output capacitances of switches M1 and IG2 and capacitor Cr keep discharging during this mode. The current in the auxiliary circuit branch is equal to the sum of the current from the full-bridge caused by the discharging of the switch output capacitances and Cr, and the input current that flows through Lsr.

$$-V_c(t) + L \frac{di(t)}{dt} + V_{in} = 0 \quad (7)$$

$$V_c = \left(I_{in} \sqrt{\frac{L}{c}} + \frac{V_0}{N} - V_{in} \right) \cos(\omega(t - t_0)) + V_{in} \quad (8)$$

$$V_c = C\omega \left(I_{in} \sqrt{\frac{L}{c}} + \frac{V_0}{N} - V_{in} \right) \sin(\omega(t - t_0)) \quad (9)$$

Mode 6: ($t_6 < t < t_7$): At the beginning of this mode, the DC bus voltage is zero and is clamped to zero as the body-diodes of the converter switches are forward biased and start to conduct. Switches IG2 can be turned on with ZVS sometime during this mode while current is flowing through their body-diodes. Also during this mode, the current that flows through the auxiliary circuit (and thus the current through the full-bridge) begins to decrease because the voltage across the auxiliary inductor is negative as the input voltage is at one end of the circuit and the DC bus voltage is zero. The auxiliary circuit current is equal to the current through Lsa at the end of this mode, which makes the current flowing through the full-bridge to be zero. Different modes of switching operation is shown in Figure 6.

In case of three-phase full bridge three level diode-clamped converter in which the dc bus consists of four capacitors, C1, C2,. For a dc bus voltage V dc, the voltage across each capacitor is V dc /2, and each device voltage stress will be limited to one capacitor voltage level i.e. V dc/2, through clamping diodes[7], [9]-[11].

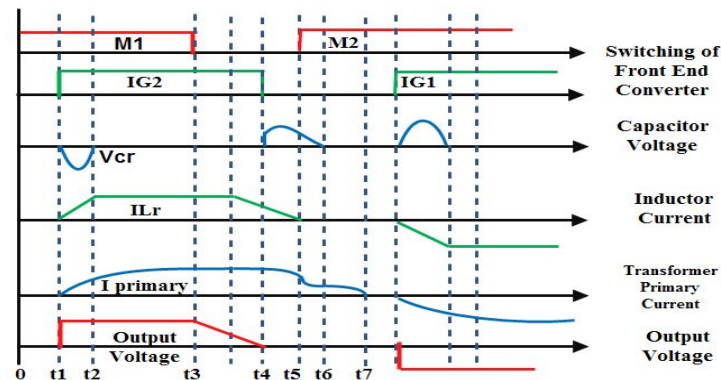


Figure 6. Different modes of operation of a Three Level Diode clamped High frequency Link Inverter

4. CONTROL TECHNIQUE

An optimized current controller is used for controlling the voltage and frequency of the inverter output voltage where the optimization of the controller is done by the Minority Charge Carrier Inspired optimization Technique (MCI). Space vector Pulse Width Modulation Technique (SVPWM) is used for pulse generation in High Frequency Link Three Phase Three Level Inverter switches. Figure 7 shows the control

diagram which is used for switching purposes. This control Technique is simple for implementation in hardware.

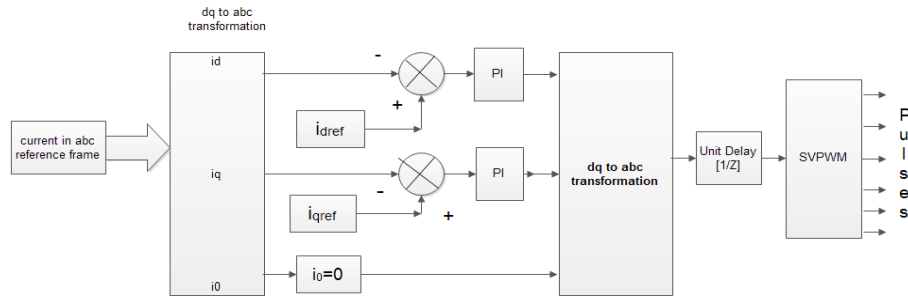


Figure 7. Control Technique and pulse generation

5. SIMULATIONS AND RESULTS

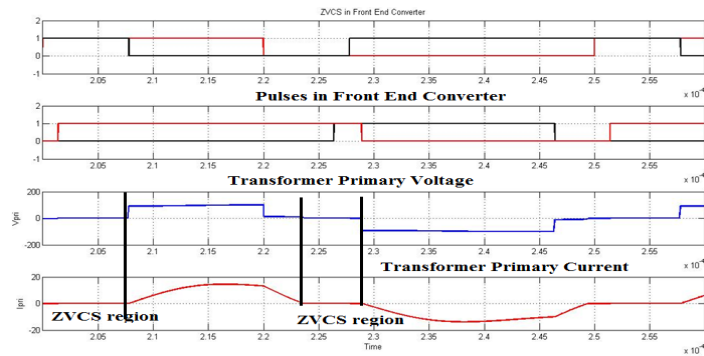


Figure 8. ZVZCS region in Front End Converter

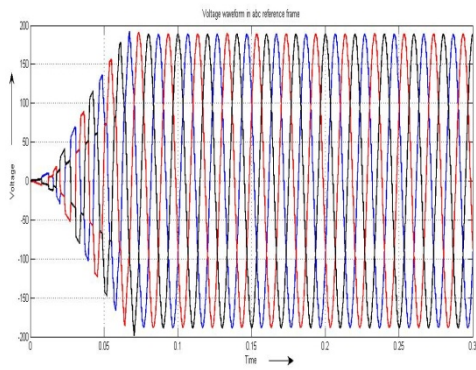


Figure 9. Voltage waveform with optimized controller

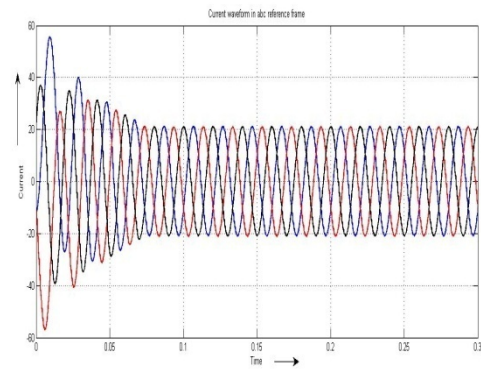


Figure 10. Current waveform with optimized controller

Figure 8 shows ZVZCS region in Front End Converter in case of ZVZCS based High Frequency Link Three Phase Three Level Diode Clamped Inverter. Figure 9 shows Grid Voltage waveform with MCI optimized Current Controller and Figure 10 shows Grid Current waveform with MCI optimized current controller.

Table 1. Stability of Voltage waveform

Type of Controller	Settling Time(sec)	Peak Overshoot (Volt)	Deviation (Volt)
I controller	0.0800	194.9	6.5
PI controller	0.0770	193.0	4.6
PID controller	0.0742	192.8	4.4

Table 2. Stability of Current waveform

Type of Controller	Settling Time(sec)	Peak Overshoot (Volt)	Deviation (Volt)
I controller	0.0770	55.38	34.45
PI controller	0.0770	55.30	34.37
PID	0.0736	55.15	34.22

From Table 1 and Table 2 One can clearly state that Optimized PID controller has the best response among all other controllers used.

6. CONCLUSION

This system has been shown to achieve the best results with high conversion efficiency, though DC-AC-DC-AC conversion is required for this result. This study was carried out for grid connections of photovoltaic and can be extended to further. Further work can be carried out to validate the practical results with the theoretical results.

REFERENCES

- [1] Ilves K, Antonopoulos A, Norrga S, Nee HP. Steady-State Analysis of Interaction between Harmonic Components of Arm and Line Quantities of Modular Multilevel Converters. *Power Electronics, IEEE Transactions on*. 2012; 27(1): 57-68.
- [2] Nguyen MK, Lim YC, Kim YJ. A Modified Single-Phase Quasi-Z-Source AC-AC Converter. *Power Electronics, IEEE Transactions on*. 2012; 27(1): 201-210.
- [3] Jung JH. Feed-Forward Compensator of Operating Frequency for APWM HB Flyback Converter. *Power Electronics, IEEE Transactions on*. 2012; 27(1): 211-223.
- [4] Han Y, Cheung G, Li A, Sullivan CR, Perreault DJ. Evaluation of Magnetic Materials for Very High Frequency Power Applications. *Power Electronics, IEEE Transactions on*. 2012; 27(1): 425-435.
- [5] Pou J, Zaragoza J, Ceballos S, Saeedifard M, Boroyevich D. A Carrier-Based PWM Strategy with Zero-Sequence Voltage Injection for a Three-Level Neutral-Point-Clamped Converter. *Power Electronics, IEEE Transactions on*. 2012; 27(2): 642-651.
- [6] Li HY, Chen HC. Dynamic Modeling and Controller Design for a Single-Stage Single-Switch Parallel Boost-Flyback-Flyback Converter. *Power Electronics, IEEE Transactions on*. 2012; 27(2): 816-827.
- [7] Baraia I, Barrena, J Abad, G Canales Segade, J Iraola, U. An Experimentally Verified Active Gate Control Method for the Series Connection of IGBT/Diodes. *Power Electronics, IEEE Transactions on*. 2012; 27(2): 1025-1038.
- [8] Mousavi A, Das P, Moschopoulos G. A Comparative Study of a New ZCS DC-DC Full-Bridge Boost Converter with a ZVS Active-Clamp Converter. *Power Electronics, IEEE Transactions on*. 2012; 27(3): 1347-1358.
- [9] Alonso JJ, Perdigão MS, Vaquero D, Calleja AJ, Saraiva E. Analysis, Design, and Experimentation on Constant-Frequency DC-DC Resonant Converters with Magnetic Control. *Power Electronics, IEEE Transactions on*. 2012; 27(3): 1369-1382.
- [10] Seong H, Kim H, Park K, Moon G, Youn M. High Step-Up DC-DC Converters Using Zero-Voltage Switching Boost Integration Technique and Light-Load Frequency Modulation Control. *Power Electronics, IEEE Transactions on*. 2012; 27(3): 1383-1400.
- [11] Lin R, Chen Y, Chen Y. Analysis and Design of Self-Oscillating Full-Bridge Electronic Ballast for Metal Halide Lamp at 2.65-MHz Operating Frequency. *Power Electronics, IEEE Transactions on*. 2012; 27(3): 1589-1597.
- [12] Chen W, Ron Hui SS. Elimination of an Electrolytic Capacitor in AC/DC Light-Emitting Diode (LED) Driver Input Power Factor and Constant Output Current. *Power Electronics, IEEE Transactions on*. 2012; 27(3): 1598-1607.
- [13] Arias M, Lamar DG, Linera FF, Balocco D, Aguisa Diallo A, Sebastián J. Design of a Soft-Switching Asymmetrical Half-Bridge Converter as Second Stage of an LED Driver for Street Lighting Application. *Power Electronics, IEEE Transactions on*. 2012; 27(3): 1608-1621.
- [14] Thielemans S, Ruderman A, Reznikov B, Melkebeek J. Improved Natural Balancing With Modified Phase-Shifted PWM for Single-Leg Five-Level Flying-Capacitor Converters. *Power Electronics, IEEE Transactions on*. 2012; 27(4): 1658-1667.
- [15] L Jia, SK Mazumder. A loss-mitigating scheme for dc/pulsating-dc converter of a high frequency-link system. *IEEE Transactions on Industrial Electronics*. 2012; 59(12): 4537-4544.

- [16] SK Mazumder, A Rathore. Primary-side-converter-assisted soft-switching scheme for an ac/ac converter in a cycloconverter-type high-frequency-link inverter. *IEEE Transactions on Industrial Electronics*. 2011; 58(9): 4161-4166.
- [17] SK Mazumder, R Burra, R Huang, M Tahir, K Acharya, G Garcia, S Pro, O Rodrigues, E Duheric. A high-efficiency universal grid-connected fuel-cell inverter for residential application. *IEEE Transactions on Power Electronics*. 2010; 57(10): 3431-3447.
- [18] R Huang, SK Mazumder. A soft switching scheme for multiphase dc/pulsating-dc converter for three-phase high-frequency-link PWM inverter. *IEEE Transactions on Power Electronics*. 2010; 25(7): 1761-1774.
- [19] M Veerachary. Power Tracking for Nonlinear PV Sources with Coupled Inductor SEPIC Converter. *IEEE Transactions on Aerospace and Electronic Systems*. 2005; 41(3).
- [20] H Altas, AM Sharaf. A Photovoltaic Array Simulation Model for Matlab-Simulink GUI Environment. *IEEE, Clean Electrical Power, International Conference on Clean Electrical Power (ICCEP '07)*. Ischia, Italy. 2007.
- [21] S Chowdhury, SP Chowdhury, GA Taylor, YH Song. Mathematical Modeling and Performance Evaluation of a Stand-Alone Polycrystalline PV Plant with MPPT Facility. *IEEE Power and Energy Society General Meeting - Conversion and Delivery of Electrical Energy in the 21st Century*. Pittsburg, USA. 2008.
- [22] Jee-Hoon Jung, S Ahmed. Model Construction of Single Crystalline Photovoltaic Panels for Real-time Simulation. *IEEE Energy Conversion Congress & Expo*. Atlanta, USA. 2010.
- [23] T Esram, PL Chapman. Comparison of photovoltaic array maximum power point tracking techniques. *IEEE Trans. Energy Convers.* 2007; 22(2): 439-449.
- [24] A Pandey, N Dasgupta, AK Mukerjee. Design issues in implementing MPPT for improved tracking and dynamic performance. *Proc. IEEE IECON*. 2006: 4387-4391.
- [25] K Noppadol, W Theerayod, S Phaophak. FPGA implementation of MPPT using variable step-size P&O algorithm for PV applications. *Proc. ISCIT*. 2006: 212-215.
- [26] M Sreedhar, NM Upadhyay, S Mishra. Optimized solutions for an optimization technique based on minority charge carrier inspired algorithm applied to selective harmonic elimination in induction motor drive. *Recent Advances in Information Technology (RAIT), 1st International Conference on*. 3012; 788-793.
- [27] Sreedhar, Madichetty, Dasgupta A. Experimental verification of Minority Charge Carrier Inspired Algorithm applied to voltage source inverter. *Power Electronics (IICPE), IEEE 5th India International Conference on*. 2012; 1-6.
- [28] Sreedhar, Madichetty, Dasgupta A. Modelling And Simulation Of A Hysteresis Band Pulse Width Modulated Current Controller Applied To A Three Phase Voltage Source Inverter By Using Mat lab. *International Journal of Advanced Research in Elec*. 2013: 4378-4387.
- [29] Soumyadeep Ray, Sreedhar Madichetty, Abhijit Dasgupta. ZVCS Based High Frequency Link Grid Connected SVPWM Applied Three Phase Three Level Diode Clamped Inverter for Photovoltaic Applications. *IEEE Power and Energy System Conference: Towards Sustainable Energy, PESTSE*. 2014: 1-6.
- [30] Sreedhar Madichetty, Soumyadeep Ray, Abhijit Dasgupta. Harmonic Mitigated Front End Three Level Diode Clamped High Frequency Link Inverter by Using MCI Technique. *International Journal of Power Electronics and Drives System*. 2014; 4(1): 91-99.
- [31] Sreedhar Madichetty, Abhijit Dasgupta. Modular Multilevel Converters Part-I: A Review on Topologies, Modulation, Modeling and Control Schemes. *International Journal of Power Electronics and Drives System*. 2014; 4(1): 36-50